Molecular Epitopes of the Ankyrin−Spectrin Interaction[†]

Jonathan J. Ipsaro,[‡] Lei Huang,[‡] Lucy Gutierrez,[§] and Ruby I. MacDonald*

Department of Biochemistry, Molecular Biology, and Cell Biology, Northwestern University, Evanston, Illinois 60208

Received December 23, 2007; Revised Manuscript Received April 8, 2008

ABSTRACT: Isoforms of ankyrin and its binding partner spectrin are responsible for a number of interactions in a variety of human cells. Conflicting evidence, however, had identified two different, non-overlapping human erythroid ankyrin subdomains, Zu5 and 272, as the minimum binding region for β-spectrin. Complementary studies on the ankyrin-binding domain of spectrin have been somewhat more conclusive yet have not presented binding in terms of well-phased, integral numbers of spectrin repeats. Thus, the objective of this study was to clearly define and characterize the minimal ankyrin−spectrin binding epitopes. Circular dichroism (CD) wavelength spectra of the aforementioned ankyrin subdomains show that these fragments are 30−60% unstructured. In contrast, human erythroid β-spectrin repeats 13, 14, 15, and 16 (prepared in all combinations of two adjacent repeats) demonstrated proper folding and stability as determined by CD and tryptophan wavelength and heat denaturation scans. Native polyacrylamide gel electrophoresis (PAGE) gel shifts as well as affinity pull-down assays implicated Zu5 and β-spectrin repeats 14−15 as the minimum binding epitopes. These results were confirmed by analytical ultracentrifugation to sedimentation equilibrium by which a 1:1 complex was obtained if and only if Zu5 was mixed with β-spectrin constructs containing repeats 14 and 15 in tandem. Surface plasmon resonance yielded a K_D of 15.2 nM for binding of β-spectrin fragments to the ankyrin subdomain Zu5, accounting for all of the binding observed between the intact molecules. Collectively, these results show the 14th and 15th β-spectrin repeats comprise the minimal, phased region of β-spectrin, which binds ankyrin at the Zu5 subdomain with high affinity.

Stress on the human red cell membrane, particularly during passage of the red cell through capillaries, is relieved by transmission to the underlying skeletal protein network (*1*). As a result, interprotein connections between the membrane and the skeletal network, termed "vertical" (*2*), as opposed to interprotein connections within the skeletal network, termed "horizontal" (*2*), are crucial to cell deformability and integrity. The vertical connections consist of two different "bridges" of proteins: one from the integral membrane protein glycophorin C to a protein complex (band 4.1, spectrin, and Actin) (*3*) in the skeletal network and a second from the anion-exchange transporter band 3 in the membrane via the adaptor protein ankyrin directly to β-spectrin in the skeletal network (*4*). A lack of effect on red cell mechanical properties upon severing the former glycophorin-containing bridge (*5*), however, speaks to a greater importance of the ankyrin-containing bridge, which is demonstrable in red cell ghosts by single particle tracking and with optical tweezers (*6*).

Most isoforms of ankyrin are comprised of an 89 kDa N-terminal membrane protein binding domain, a central 62 kDa spectrin-binding domain, and a 55 kDa C-terminal regulatory domain (*4*) (Figure 1). Much is known about the associations of the multiple isoforms of this ubiquitous protein (*7, 8*), the static and kinetic properties of the ankyrin−band 3 interaction (*9*), and the consequences of ankyrin mutations for cardiac and other functions (*10, 11*). Characterization of its molecular structure, however, has been confined largely to its band 3 binding domain of so-called ankyrin repeats. An X-ray crystal structure of a fragment of repeats (*12*) suggests origins of its spring-like behavior, which were later demonstrated by atomic force microscopy (*13*).

In comparison with progress on the membrane protein binding domain, structural information for the spectrin-binding domain (SpBD)[1] and the regulatory domain of ankyrin is meager. Given its critical role as part of the bridge

[†] This work was supported by National Institutes of Health (NIH) Grant GM 57692 to R.I.M.

* To whom correspondence should be addressed. Telephone: (847) 309-2707. Fax: (847) 467-1380. E-mail: rubymacd@northwestern.edu.

[‡] These authors contributed equally to this study.

[§] Present address: 2443 W. Sunnyside, Number 3, Chicago, IL 60625.

[1] Abbreviations: AEBSF, 4-(2-aminoethyl) benzenesulfonyl fluoride hydrochloride; AUC, analytical ultracentrifugation; CBα, chicken brain α-spectrin; CD, circular dichroism; DTT, dithiothreitol; EDTA, ethylenediaminetetracetic acid; ESI, electrospray ionization; HEβ, human erythroid β-spectrin; HEPES, 4-(2-hydroxyethyl)-1-piperazineethanesulfonic acid; HSQC, heteronuclear single-quantum coherence; IAEDANS, 5-[([(2-iodoacetyl)amino]ethyl)amino]-naphthalene-1-sulfonic acid; IPTG, isopropyl-β-D-1-thiogalactopyranoside; ITC, isothermal titration calorimetry; LB, Luria−Bertani medium; NMR, nuclear magnetic resonance; NRMSD, normalized root-mean-square difference; PAGE, polyacrylamide gel electrophoresis; PCR, polymerase chain reaction; PED(P), 20 mM sodium phosphate at pH 8.0, 1 mM EDTA, and 1 mM DTT (0.1 mM PMSF); PE/PC, phosphatidylethanolamine/phosphatidylcholine; PMSF, phenylmethylsulfonyl fluoride; Q-TOF, quadrupole time-of-flight; RU, response unit; SDS−PAGE, sodium dodecyl sulfate−polyacrylamide gel electrophoresis; SpBD, spectrin-binding domain; SPR, surface plasmon resonance; TCEP, tris(2-carboxy-ethyl)phosphine hydrochloride; TEDP, 20 mM Tris at pH 8.0, 1 mM EDTA, 1 mM DTT, and 0.1 mM PMSF; TEV, tobacco etch virus; UV, ultraviolet.

10.1021/bi702525z CCC: $40.75
Published on Web 06/19/2008

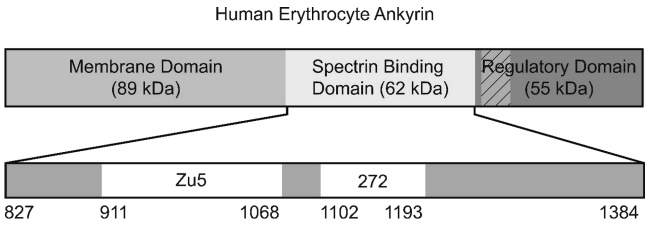

FIGURE 1: Diagram of human erythrocyte ankyrin. The three domains of ankyrin (N-terminal membrane domain, spectrin-binding domain, and C-terminal regulatory domain) are diagrammed to scale. The hatched region within the 55 kDa regulatory domain indicates the location of a ~10 kDa death domain. (Below) Magnification of the spectrin-binding domain (SpBD) indicates the positions and sizes of the putative minimal binding regions, Zu5 and 272. Corresponding amino acid residue numbers for the SpBD are provided.

directly tethering the skeletal network to the cell membrane, SpBD is particularly crucial during reversible deformation of red cells. To address the molecular properties of this force-transmitting site, questions as to the identity of the molecular epitope(s) of ankyrin interacting with spectrin needed to be resolved. A spectrin-binding epitope within SpBD, originally identified by Wallin et al. (*14*), was first reported to be "272" (*15*), according to immunoblot binding of SpBD fragments to biotinylated spectrin and to competition between fusion proteins and ankyrin for radiolabeled spectrin on inside-out red cell vesicles. More recently, a non-overlapping SpBD peptide sequence containing a Zu5 domain plus 55 residues C-terminal to it, herein referred to as "Zu5", was reported to be a β2-spectrin-binding epitope from results of yeast 2-hybrid assays (*16*). According to Zhang et al. (*17*), Zu5 is a "functionally unknown domain found in ZO-1 and UNC5H receptors".

The first portion of this study was begun to identify the molecular epitope(s) of ankyrin involved in binding spectrin (*15, 16*). The results presented here show that the Zu5 subdomain binds specifically to fragments containing β-spectrin repeats 14 and 15 according to a native polyacrylamide gel-shift assay, affinity pull-downs, as well as analytical ultracentrifugation to sedimentation equilibrium. In contrast, 272 did not evidence binding by any of these methods. To complement the information gathered regarding the minimal spectrin-binding regions of ankyrin, similar studies were performed with the ankyrin-binding domain of spectrin. While there has been less controversy over the regions of spectrin implicated in binding, structural studies of other spectrin repeats have revealed the necessity for proper "phasing" of cloned spectrin repeats.

The 37 triple-helical repeats of the repeating unit domain of the α- and β-spectrin heterodimer are often represented in diagrams by identical symbols (Figure 2). This implication of identity has been heuristically useful for measuring (*18*) mechanical properties of the red cell skeletal network, although recent protein-unfolding studies suggest heterogeneity among repeats with respect to their stabilities of folding (*19, 20*) and melting temperatures (*21*). More obvious functional correlates of this heterogeneity are the specific affinities of certain spectrin repeats reviewed by Djinovic-Carugo et al. (*22*), which indicate that the low (20−30%) amino acid sequence identity among repeats (*23*) has evolved to afford functional specialization within the repeating unit domain of spectrin. This reasoning also applies, of course, to the other prominent members of the spectrin family, α-actinin and dystrophin (*24*). It remains a mystery, however, as to what dictates this structural versatility of the signature spectrin-repeating unit motif (*25*) despite the availability of X-ray crystal structures of two (*19, 26, 27*) and three (*28*) repeat fragments of spectrin and α-actinin.

The specialization of interest here is the affinity of certain spectrin fragments for the adaptor protein ankyrin. A minimal version of the ankyrin-binding subdomain had originally been identified as β-spectrin repeat 15 by cloning and testing of incrementally smaller regions of the C-terminal end of β-spectrin for binding to inside-out red cell vesicles (*29*). However, it became apparent subsequently that this "repeat 15" was actually the C-terminal third of repeat 14 plus the whole of repeat 15, encompassing the start and stop sites of canonical spectrin repeats defined by surveying the circular dichroism (CD) spectra and protease sensitivities of differently phased fragments (*30*). Nevertheless, the identity of this region as the ankyrin-binding site is supported by its harboring (1) a sequence in the 15th repeat, which is well-conserved among β-spectrins I, II, and III with ankyrin-binding activity and (2) a 43 residue region of low homology with other repeats (*31*). Four cloned permutations of repeat 15 were recently reported to yield somewhat different results, depending upon whether ankyrin-binding activity was assayed by interaction with intact ankyrin, interaction with a phosphatidylethanolamine/phosphatidylcholine (PE/PC) monolayer, binding to PE/PC liposomes, or inhibition of spectrin binding to PE/PC liposomes (*32*). Perhaps because of slight differences in phasing of start and stop sites, ankyrin-binding activity was obtained with a fragment missing the C-terminal half of β-spectrin repeat 15 (*32*), which had been previously found to be necessary (*29*).

To determine which repeats are minimally necessary for binding to the spectrin-binding subdomain of ankyrin, three two-repeat fragments of β-spectrin, HEβ1314, HEβ1415, and HEβ1516, and one three-repeat fragment, HEβ1315, were cloned. With concern for physiological relevance of the results in the present study, these four β-spectrin fragments were designed to conform to the start and stop sites of a canonical, 106 amino acid spectrin repeat (*30*), although 6 residues were added to the N and C termini of HEβ1415 and 2 residues to the N and C termini of HEβ1315 to minimize "fraying". Such small additions have been shown to enhance the stabilities of folding of spectrin (*33*) repeats. Furthermore, in addition to CD and tryptophan fluorescence spectra, free energies of heat-induced unfolding, i.e., ΔG values, were determined for evaluation of the stabilities of folding of the candidate peptides. Finally, these phased and well-folded fragments were tested for binding to tagged and untagged versions of the Zu5 plus neighboring 55 residue subdomain of the SpBD of ankyrin, previously reported to exhibit spectrin-binding activity *in vivo* (*16, 34*). Among the tested fragments, only β-spectrin fragments containing repeats 14 and 15 were able to bind the subdomain of ankyrin "Zu5", in agreement with the earlier finding that ankyrin-binding activity requires both the C-terminal third of repeat 14 and the whole of repeat 15 (*29*). Binding measurements indicated a K_D of ~15 nM, suggesting these minimal binding regions are responsible for nearly all of the binding observed between the intact molecules (*35*). When these results are taken together, they provide for the first time a promising

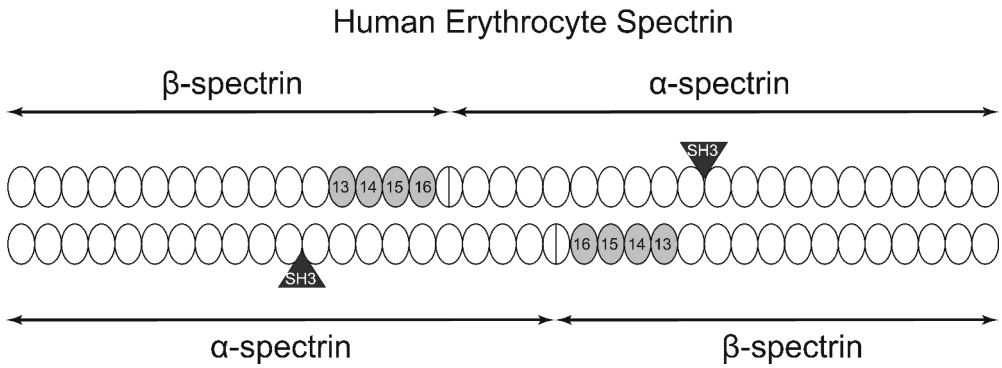

FIGURE 2: Diagram of the human erythrocyte spectrin tetramer. The human erythrocyte spectrin tetramer consists of two α and two β chains, arranged as shown. Each spectrin repeat of the tetramer is depicted as an ellipse; repeats of interest in studying spectrin−ankyrin binding (13−16) are shaded and numbered. Divided ellipses represent the dimerization sites formed from the N terminus of α-spectrin and the C terminus of β-spectrin. Triangles indicate the SH3 domain of α-spectrin.

system for determining the molecular basis of this affinity, which is critical to the reversible deformation of red cells.

EXPERIMENTAL PROCEDURES

Preparation of Ankyrin Constructs. cDNA coding for both ankyrin peptides, Zu5 (residues 911−1068) (*16*) and 272 (residues 1102−1193) (*15*), was human erythroid ankyrin cDNA Ank15 kindly given by Dr. Patrick Gallagher (*36, 37*). Zu5 and 272 were cloned into pET-3c and pET-30b, respectively, by amplifying the target sequences via polymerase chain reaction (PCR), gel purifying the PCR products, and ligating them into the target vector. *Escherichia coli* DH5α cells were transformed with the recombinant plasmids by electroporation and plated on Luria−Bertani medium (LB) agar with the appropriate antibiotics. After overnight incubation at 37 °C, single colonies were cultured for plasmid amplification followed by DNA miniprep purification (Promega Wizard kit). To ensure fidelity of cloning and to verify construct identity, each was sequenced by the Northwestern University Sequencing Facility.

Preparation of Spectrin Constructs. cDNA coding for spectrin constructs was human erythroid β-spectrin (HEβ) cDNA (*38*) and chicken brain α-spectrin (CBα) cDNA (*39*), kindly provided by Dr. Bernard Forget and the late Dr. Matti Saraste, respectively. The new target constructs, HEβ1314 (residues 1586−1798), HEβ1415 (residues 1686−1910), HEβ1516 (residues 1799−2010), and HEβ1315 (residues 1584−1906), were PCR-amplified for cloning into the ligation-independent vector pMCSG7 (*40*). Sizes of the PCR products were verified by agarose gel electrophoresis and the amplified DNA products purified (Qiagen gel extraction kit). Exonuclease treatment for incorporation into the vector was performed according to Stols et al. (*40*). The recombinant plasmids were transformed into *E. coli* NovaBlue competent cells (Novagen) by heat shock and plated on LB agar with 100 μg/mL ampicillin. Plasmid isolation and sequence were performed as described above. Cloning and preparation of HEβ89 in pET-23d and CBα1617 in pET-3d were completed as previously described (*19, 20, 27*).

Protein Expression of Zu5. E. coli Rosetta2(DE3) competent cells (Novagen) were transformed by heat shock and plated on LB agar containing 100 μg/mL ampicillin and 34 μg/mL chloramphenicol. After overnight incubation at 37 °C, single colonies were inoculated into 50 mL of LB with antibiotics and grown for ∼16 h at 37 °C with shaking. The starter cultures were then transferred to 1 L LB cultures and incubated at 37 °C with shaking until the OD_{600} was 0.5. The cultures were briefly cooled, and protein expression was induced with 0.5 mM isopropyl-β-D-1-thiogalactopyranoside (IPTG). Cultures were then incubated overnight at 16 °C with shaking. Cells were harvested by centrifugation at 6000 rpm, and the cell pellet was stored at −80 °C.

Protein Expression of 272. Expression of 272 was carried out as described for Zu5, except that 50 μg/mL kanamycin was used in each step rather than ampicillin, cultures of 272 were maintained at a constant 37 °C, and protein expression was induced for 3−4 h at this temperature followed by harvesting as above.

Expression of Spectrin Constructs. Recombinant plasmids bearing cDNA for β-spectrin repeats were transformed into *E. coli* BL21(DE3) by heat shock and grown on LB agar plates containing the appropriate antibiotic. After overnight incubation at 37 °C, single colonies were inoculated into 50 mL LB media with antibiotic and grown at 37 °C with shaking at 300 rpm. After ∼16 h, this starter culture was centrifuged at 6000*g* for 15 min at 4 °C, the supernatant was removed, and the cell pellet was resuspended in 10 mL of fresh LB. The resuspended culture was then transferred to 1 L of LB with antibiotic (initial OD_{600} of ∼0.1) and incubated at 37 °C with shaking at 300 rpm. After ∼2.5 h (OD_{600} of 0.5−0.6), protein expression was induced with 1 mM IPTG for 3 h, after which the cells were harvested at 5000*g* for 30 min at 4 °C. The resulting cell pellet was frozen and stored at −80 °C.

Protein Purification of Nontagged Zu5 and 272. Frozen cell pellets from 1 L of culture were resuspended in 20 mL of PED [20 mM sodium phosphate at pH 8.0, 1 mM ethylenediaminetetracetic acid (EDTA), and 1 mM dithiothreitol (DTT)] with 1 mL protease inhibitor cocktail containing 4-(2-aminoethyl) benzenesulfonyl fluoride hydrochloride (AEBSF), EDTA, bestatin, pepstatin A, and E-64 (Sigma P8465). After five cycles of sonication (1 min on and 1 min off) at 4 °C, the cell lysate was centrifuged at 35000*g* at 4 °C for 1 h. The supernatant was loaded onto a carboxymethyl sepharose (Sigma) column pre-equilibrated with PED and then washed with 20 mL of PEDP [PED buffer with 0.1 mM phenylmethylsulfonyl fluoride (PMSF)]. A 0−0.5 M NaCl gradient in PEDP was used to elute the bound species. Fractions containing the target protein were then loaded on a S (sulfonyl) methacrylate (Bio-Rad) column and

eluted with a 0−1.0 M NaCl gradient in PEDP. When necessary, the target protein was further chromatographed on a P-10 (Bio-Rad) size-exclusion column. Zu5 and 272 were concentrated by centrifugation in Amicon Ultra centrifugal filter devices. Purity of the proteins was monitored by sodium dodecyl sulfate−polyacrylamide gel electrophoresis (SDS−PAGE) on 4−20% polyacrylamide gradient gels (Pierce), 4−12% polyacrylamide gradient gels (Invitrogen), or on 15% polyacrylamide gels, and the protein concentration was determined by $A_{\lambda=280}$ measurement and extinction coefficients calculated from ultraviolet (UV) absorbing amino acids in the sequences.

Expression and Purification of His-Tagged Ankyrin Constructs. Protein expression of the His-tagged ankyrin constructs and cell lysis were performed as described for their nontagged counterparts. After centrifugation, the resulting supernatant was first purified by affinity chromatography on Ni-CAM resin (Sigma). Subsequent S (sulfonyl) methacrylate (Bio-Rad) column and P-10 (Bio-Rad) size-exclusion column purification were also performed as described above. When necessary, Zu5 and 272 were concentrated with Amicon Ultra centrifugal filter devices. The purity of the proteins was monitored by SDS−PAGE on 4−20% polyacrylamide gradient gels (Pierce).

Purification of Spectrin Constructs. After thawing, cells were resuspended in 20 mL of 50 mM sodium phosphate at pH 8.0 and 10 mM imidazole and lysed by five cycles of sonication (1 min on and 1 min off). Cell debris was then removed by centrifugation at 35000*g* for 30 min. For His-tagged constructs, the resulting supernatant was purified by affinity chromatography on Ni-CAM resin (Sigma). Subsequently, the His tag was removed with TEV protease (1:20 m/m ratio construct/protease) at 4 °C for ∼20 h while simultaneously dialyzed into 50 mM sodium phosphate at pH 8.0. TEV protease and any remaining uncleaved protein were removed with Ni-CAM resin. Untagged constructs were purified as described previously (*20, 27*). Ion-exchange chromatography on Q-Sepharose (Sigma) and size-exclusion chromatography on S-100 (Bio-Rad) were then carried out for all target proteins in TEDP-based buffers (20 mM Tris at pH 8.0, 1 mM EDTA, 1 mM DTT, and 0.1 mM PMSF). Fractions were tested by SDS−PAGE; those which contained protein of the highest purity and in highest yield were pooled and further purified. The resulting purified proteins were desalted into 10 mM HEPES at pH 7.5 on a 10DG desalting column (Bio-Rad), concentrated to ∼200 μM, and stored at 4 °C. Typical yields ranged from 5−50 mg of purified protein per liter of culture. The protein concentration was determined from absorbance at 280 nm and calculated extinction coefficients.

CD. CD measurements were obtained with a Jasco J715 spectropolarimeter equipped with a Peltier device and calibrated with *d*-10-camphorsulfonic acid (Keck Facility, Northwestern University). The data pitch was 1 nm; the scan speed was 20 nm/min; the response time was 8 s; and the bandwidth was 1 nm. Wavelength scans of Zu5 at room temperature and 272 at 6 °C were performed in buffer containing 10 mM sodium phosphate at pH 8.0, 0.14 M NaF, and 1 mM tris(2-carboxy-ethyl)phosphine hydrochloride (TCEP) using a 0.2 mm path-length demountable cuvette. Wavelength scans of spectrin fragments at room temperature were carried out at a final protein concentration of 15−20 μM in 10 mM sodium phosphate at pH 8.0 and 0.14 M NaF (0.2 mm path-length demountable cuvette). Heat-denaturation scans (final protein concentration of 1 μM in a 1 cm cuvette) were measured at 222 nm from 10 to 85 °C. Samples were heated at a rate of 1 °C/min with stirring. Data for wavelength scans are given after buffer subtraction and presented in units of molar ellipticity ([θ]), deg cm^2 dmol^{-1}.

Tryptophan Fluorescence. Purified spectrin fragments were diluted to 4−6 μM in 10 mM sodium phosphate at pH 8.0 and 0.14 M NaCl. Samples in 0.5 cm square quartz cuvette were excited at 295 nm, and emission scans from 300 to 380 nm were collected with a Hitachi F-4500 fluorescence spectrometer. Slit widths of 5 nm were used throughout.

Thermodynamic Analysis of Thermal Unfolding. Stabilities of folding based on CD-monitored thermal unfolding were determined as previously described (*28, 33*). Buffer-subtracted spectra were fit with SigmaPlot 8.0 to equations describing two- (*33*) or three-state (*28*) transitions to yield transition temperatures (T_M) and slopes of the transition (ΔT). Free energies of unfolding, ΔG, at 25 °C were obtained from eq 1

$$\Delta G = 4RT_M(T_M - T)/\Delta T \quad (1)$$

where R is the gas constant of 1.987 cal K^{-1} mol^{-1} and T is 298 K.

Gel-Shift Assay. The indicated proteins were mixed in a 1:1 molar ratio, except where noted for stoichiometry determination, and incubated on ice for 15 min before loading of the gel. The 10% polyacrylamide gels (with 5% stacking gel when indicated) at pH 7.4 (*41*) were prerun for 30 min at 30 V before loading. Samples were mixed with 6× loading buffer (40% sucrose) and run at 30 V for roughly 4 h at 4 °C (measured gel running temperature was 4.6 °C). Protein was visualized by Coomassie Blue staining.

Analytical Ultracentrifugation to Sedimentation Equilibrium. Sedimentation equilibrium experiments with Zu5 and 272 were carried out in a Beckman XL-A analytical ultracentrifuge at 20 and 6 °C, respectively, in 10 mM sodium phosphate at pH 8.0, 0.1 M NaCl, and 1 mM EDTA. A total of 130 μL of sample from 0.25 to 0.52 mg/mL were centrifuged at 20 000 rpm for 24 h, and scans were taken at 18 and 24 h to establish attainment of the equilibrium. Where indicated, additional scans at 35 000 and 48 000 rpm were taken sequentially; samples were allowed 12 h to reach equilibrium before scanning at each of these higher speeds. Concentration distributions were measured at 280 nm and determined on SedPhat (version 4.4b) (http://www.analyticalultracentrifugation.com/sedphat/sedphat.htm) by fitting the data to equations describing single-ideal, two-ideal, nonideal, or association models. Correspondence between the data and the calculated fit, randomness of residuals, and global reduced χ^2 values close to 1 were used to assess the quality of the fit.

Mass Spectrometry. Purified proteins were diluted in water to 0.25−2.5 μM and applied to a Phenomenex Jupiter Proteo column (1.0 × 150 mm, 4 μm particle size) at 50 μL/min. In total, ∼1 pmol (4 μL) of material was injected. A mobile-phase gradient from 0.1% formic acid in water to 0.08% formic acid in acetonitrile was used to chromatograph each sample over 6 min, which was then taken for in-line electrospray ionization−mass spectrometry (ESI−MS). Mass spectra were obtained on an Agilent 6510 Accurate-Mass

Q-TOF LC/MS with an accelerating voltage of 4100 V. Deconvolution was performed with the included software, Agilent MassHunter Qualitative Analysis, version B.01.02. Masses of all proteins were within 1.0 Da of those predicted.

Surface Plasmon Resonance (SPR). Binding affinities and kinetics of biotinylated spectrin fragments to Zu5 were measured with a Biacore 3000 equipped with a streptavidin biosensor. Prior to immobilization, three purified spectrin fragments (HEβ1315, HEβ1415, and CBα1617) were individually biotinylated. Each of these constructs contained a single cysteine near the C terminus, which allowed for directed biotinylation with 1-biotinamido-4-[4′-(maleimidomethyl)cyclohexanecarboxamido]butane (Pierce, protocol of the manufacturer was followed). The biotinylated spectrins (ligands) were diluted in HBS-P [10 mM HEPES at pH 7.4, 0.15 M NaCl and 0.005% (v/v) surfactant P20, Biacore] to a final concentration of 1 nM and applied to individual flow cells of a streptavidin-modified biosensor (sensor chip SA, GE Healthcare) at a rate of 20 μL/min at 25 °C. Between 100 and 150 response units (RUs) were immobilized for each biotinylated ligand. Immobilization was judged to be stable, with no noticeable decay in response. Purified Zu5 (analyte) in HBS-P was diluted serially to the concentrations indicated and maintained at 10 °C until the time of injection. Injections were performed in parallel, with Zu5 being applied over all flow cells simultaneously at a flow rate of 20 μL/min and a sensor temperature of 25 °C. Injections were performed in triplicate using HBS-P as the system buffer; association and dissociation phases were 60 s each. Zu5 completely dissociated after ~180 s; nevertheless, a 300 s postdissociation phase wash was included in the run parameters to ensure complete removal of Zu5 from previous injections. Data were analyzed using the included BIAevaluation software (version 4.1). Sensorgrams for each set of injections were processed globally (and simultaneously for k_a and k_d) after reference cell and buffer subtraction. Fits were assessed by correspondence between the data and the calculated fit, randomness of residuals, and nearness of global reduced χ^2 values to 1.0. Values presented for the k_a, k_d, and K_D (calculated by k_a/k_d) represent the average ± average standard deviation for the three replicates for each ligand.

RESULTS

Isolation of Ankyrin Subdomains Zu5 and 272. Two neighboring but non-overlapping subdomains of the SpBD of human erythroid ankyrin (Figure 1) were previously reported to be minimally necessary to interact with the ankyrin binding site on human erythroid β-spectrin: (i) "Zu5," a 17 588 Da peptide of 158 residues (*16*), and (ii) "272," a 10 187 Da peptide of 92 residues (*15*). These two different molecular epitopes putatively involved in spectrin binding had been cloned and tested largely as proteolyzed peptide fragments in immunoblot assays with biotinylated spectrin or as fusion proteins competing with ankyrin on inside-out red cell vesicles for radiolabeled spectrin (*15*) or in yeast two-hybrid assays (*16*). With the goal of eventual structure determination of the spectrin−ankyrin binding site crucial to red cell skeletal integrity, it became necessary for us to clone, isolate, and study these candidate epitopes free of unrelated domains, which could potentially influence their conformations in a nonphysiological manner. 272 and Zu5 were cloned, expressed, and purified separately to greater than 99% purity (Experimental Procedures) as shown by SDS−PAGE in Figure 3. The DNA sequence of both proteins was found to be correct by sequencing; masses of these proteins were verified to within 1.0 Da by mass spectrometry. Properties that hindered the recovery of these proteins were the tendencies of Zu5 to become insoluble during expression and to precipitate over time, once purified, and of 272 to aggregate at temperatures greater than 4 °C.

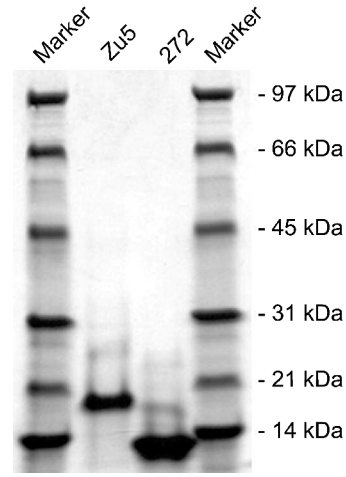

FIGURE 3: Purity and apparent molecular masses of SpBD constructs. A Coomassie Brilliant Blue-stained 4−20% SDS−PAGE gel of purified Zu5 and 272 flanked by molecular mass markers is shown.

Greater than 30% of 272 and Zu5 Are Unstructured by Modeling of Their CD Data. One reason for the above and other difficulties encountered in isolating and purifying Zu5 and 272 became apparent upon measurement of CD spectra of Zu5 (Figure 4A) and 272 (Figure 4B). Solutions of each protein in 10 mM sodium phosphate at pH 8.0 and 0.15 M NaF, with 1 mM TCEP were scanned from 250 to 185 nm and yielded a mean residue ellipticity at 222 nm of 3923 deg cm^2 dmol^{-1} residue^{-1} for Zu5 and 3267 deg cm^2 dmol^{-1} residue^{-1} for 272. The spectra were then analyzed with standard algorithms in conjunction with appropriate protein reference sets on the website DICHROWEB (*42*). The algorithm giving by far the best fit to the spectra of both Zu5 and 272 was CONTINLL (*43*), in combination with reference sets 6 and 3, respectively. These conditions gave a normalized root-mean-square difference (NRMSD) of ~0.05 and a virtually superimposable fit of the calculated spectra to the measured spectra of Zu5 (Figure 4A) and 272 (Figure 4B), whereas the next best combination of algorithm and reference set gave a NRMSD of 0.17 and a poor fit of the calculated spectra to the measured spectra (not shown). The average percentages of predicted secondary structure given in each figure are shown in Table 1.

Zu5 Forms a Complex with HEβ1315 or HEβ1415 but Not with HEβ89 or CBα1617 on Native Polyacrylamide Gels. To corroborate the specific interaction of Zu5 or 272 with HEβ1315 or HEβ1415 but not with CBα1617, each protein was subjected to native 10% PAGE (Figure 5A).

Unfortunately, 272 (pI 9.5) did not enter the gel at pH 7.4 (rightmost lane in Figure 5A) nor was an observable shift in spectrin fragment migration noted when spectrin fragments were mixed with 272 and run at pH 7.4 (not shown). Several attempts were made to demonstrate 272-containing com-

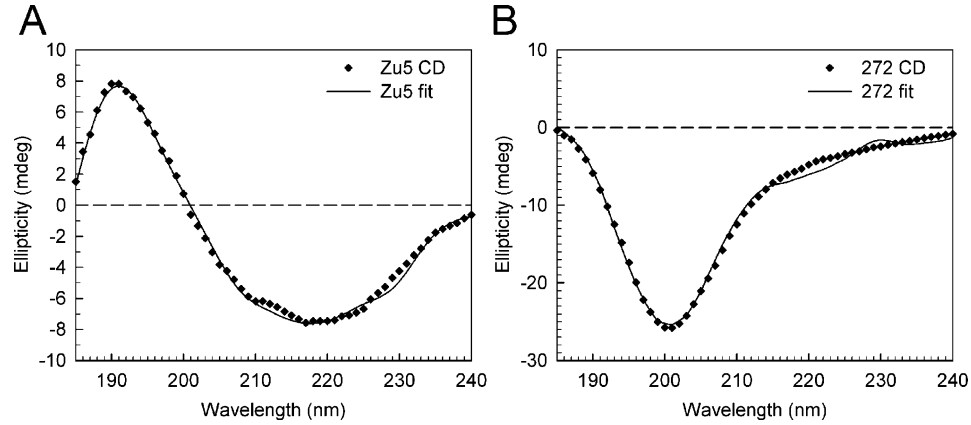

FIGURE 4: Conformational analysis by CD. (A) CD wavelength scan for Zu5 (◆) and reconstructed fit (—). (B) CD wavelength scan for 272 (◆) and reconstructed fit (—). Fitting was performed with CONTINLL and reference set 3 on DICHROWEB. NRMSD values were 0.054 and 0.050 for Zu5 and 272, respectively.

Table 1: Secondary-Structure Analysis of Ankyrin Fragments Suggests Intrinsically Unstructured Regions[a]

secondary structure	Zu5 using reference set 3 NRMSD = 0.054 (%)	272 using reference set 3 NRMSD = 0.051 (%)	272 using reference set 6 NRMSD = 0.051 (%)
α helix	7.8	19.2	7.4
β strand	39.5	16.1	22.1
turns	19.8	26.2	10.0
unstructured	32.9	38.7	60.5

[a] Secondary-structure modeling analysis of CD data by DICHROWEB for Zu5 and 272 are shown. DICHROWEB discriminates between "regular" and "distorted" forms of α helix and *β* strand, which are assigned according to the secondary-structure prediction program DSSP (*60*) but were pooled for presentation here, because the two forms are sufficiently similar for present purposes.

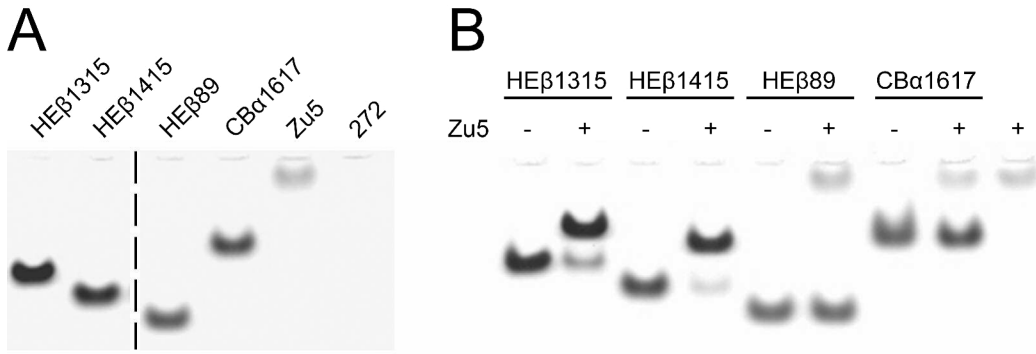

FIGURE 5: Gel-shift assays with Zu5 demonstrate binding to HE*β*1415. (A) Native 10% PAGE of all purified constructs show that the spectrin repeats, with relatively low pI values of about 4−6 migrated more quickly than Zu5 with a pI of 8.5. 272, with a pI of 9.5, failed to enter the gel when run toward the (+) anode. (B) Native 10% PAGE of HE*β*1315, HE*β*1415, HE*β*89, and CBα1617 in the presence or absence of Zu5 are shown. A noticeable shift is observed for both HE*β*1315 (lane 2) and HE*β*1415 (lane 4) but not for HE*β*89 or CBα1617. Zu5 alone is shown in the far right lane for comparison. Separate regions of the same gel are divided by a dashed line.

plexes via gel shift by varying protein ratios, adjusting the pH of the gel and running buffer (pH ranged from ~4.0 to ~8.5 in 0.5 pH unit increments), and electrophoresing in the (−) cathode direction. None of these variations demonstrated the formation of 272-containing complexes, making this assay definitive only for characterizing Zu5 binding to HE*β*1315 and HE*β*1415.

In contrast with 272, however, Zu5 was shown to form specific complexes. Figure 5B shows the gel lanes marked according to the proteins added. Zu5 alone is in the extreme right lane. The first four lanes on the left show that either HE*β*1315 or HE*β*1415 forms a complex with Zu5; the next four lanes show that neither HE*β*89 nor CBα1617 forms a complex with Zu5. In the lanes with both Zu5 and HE*β*1315 or HE*β*1415, a small amount of excess HE*β*1315 and HE*β*1415 is seen below the complexes (i.e., migrating more quickly). These conclusions were also validated using nickel-affinity pull-down (methods and results can be found in the Supporting Information).

Zu5 Forms a Complex with HEβ1315 and HEβ1415 but Not with CBα1617 at Sedimentation Equilibrium. To examine the affinities of Zu5 and 272 for the ankyrin binding site on spectrin in solution, sedimentation equilibrium experiments were performed. Plots of the 280 nm absorbance versus centrifugal radius for a representative of each sample type are shown in Figure 6, accompanied by fits and residuals.

For Zu5-containing mixtures, the single ideal species model gave the best fits with global reduced χ^2 values close to 1.0 and randomly distributed residuals. Zu5 alone (top left in Figure 6) behaved as a monomer in the absence of spectrin fragments at pH 8.0 at 6 °C. Furthermore, a molecular mass within 10% of that of a 1:1 complex was found for Zu5 with the three-repeat fragment, HE*β*1315 (top center in Figure 6) and for Zu5 with the two-repeat fragment,

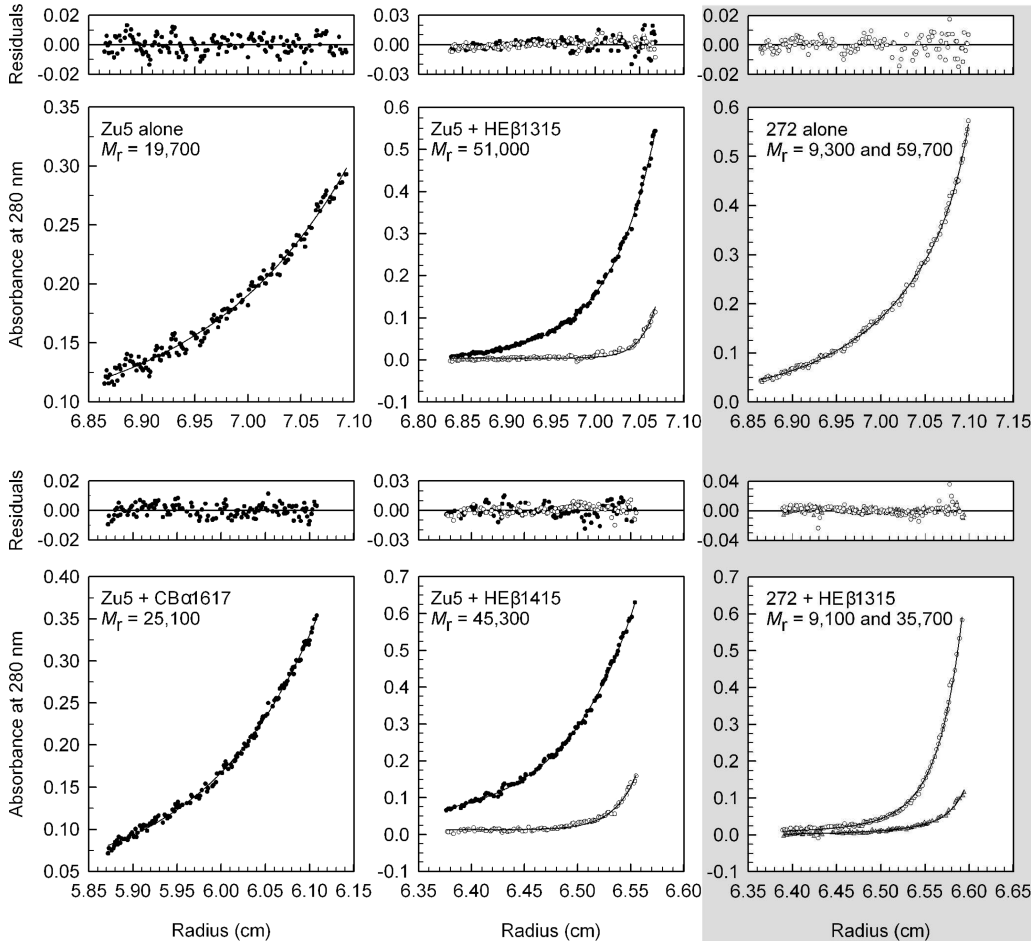

FIGURE 6: Analytical ultracentrifugation to sedimentation equilibrium indicates that Zu5 but not 272 stably binds HEβ1315 and HEβ1415. Analytical ultracentrifugation results for ankyrin constructs in the presence and absence of spectrin constructs are shown with fits and residuals. Zu5 (top left panel) exists as a monomer in solution and forms a stable complex with HEβ1315 (top center panel) and HEβ1415 (bottom center panel). To confirm the stability of this complex, data were analyzed at two speeds; the data presented show the global fit for each mixture. In contrast, Zu5 did not form a complex with CBα1617 (bottom left panel), demonstrating the specificity of complex formation. 272 (top right panel) existed in a monomer−aggregate equilibrium, which reproducibly gave molecular masses of ~10 and ~60 kDa when measured at 6 °C. The 60 kDa aggregate could be "cleared" from the sample by spinning at high speed (data not shown). Finally, 272 did not provide evidence for complex formation with HEβ1315 (bottom right panel). All data were collected at 6 °C. Filled circles indicate data collected at 20 000 rpm; open circles indicate data collected at 35 000 rpm; and shaded triangles indicate data collected at 48 000 rpm.

HEβ1415 (bottom center in Figure 6). In contrast, Zu5 with the two-repeat fragment, chicken brain α-spectrin 16 and 17 (CBα1617), yielded a molecular mass of 25.1 kDa (only 60% of a complex) (bottom left in Figure 6). Presumably, the similar mass of Zu5 alone was obscured by the fit of this sample.

In comparison, 272 (top right in Figure 6) existed in a monomer−aggregate equilibrium under the same conditions. Interestingly, this aggregation was found quite reproducibly in the 40−80 kDa range at speeds < 35 000 rpm, but at speeds > 35 000 rpm (not shown), this larger species could be "removed", presumably by pelleting the aggregated 272. Thus, data for 272 alone fit the association model at speeds < 35 000 rpm but fit the single-ideal species model at speeds > 35 000 rpm. In the presence of spectrin fragments, data for 272 fit the two ideal species model, which indicated that 272 was not binding to spectrin fragments. Data for HEβ1315 with 272 is shown in the lower right panel of Figure 6.

Finally, in view of their proximity within the SpBD, Zu5 and 272 were also tested by ultracentrifugation for simultaneous binding to HEβ1415. This experiment yielded a molecular mass that is 79% of a ternary complex but 99% of a complex of Zu5 plus HEβ1415 (not shown).

Defining the Minimum Number of β-Spectrin Repeats Interacting with the Minimum Spectrin-Binding Subdomain of Ankyrin. Progress toward identifying the ankyrin binding region of β-spectrin began with the observation that repeat 15 alone binds to ankyrin on inside-out red cell vesicles (*29*). Only upon later structural determination of spectrin repeats did it become apparent that this "repeat 15" (*29*) actually comprised the C-terminal third of repeat 14 and the whole of repeat 15, according to the phasing of start and stop sites of canonical spectrin repeats (*30*). To test well-folded spectrin fragments for binding to the ankyrin subdomain Zu5, recloning of different combinations of canonically phased, two- and three-repeat fragments in the region of the 14th and 15th repeating units of human erythroid β-spectrin was undertaken. Figure 2 indicates the locations of the 13−16th β-spectrin repeats of interest (filled ellipses) among other repeats (open ellipses) within two α- and β-spectrin dimers forming a tetramer.

In view of the greater stability of spectrin (*33*) fragments

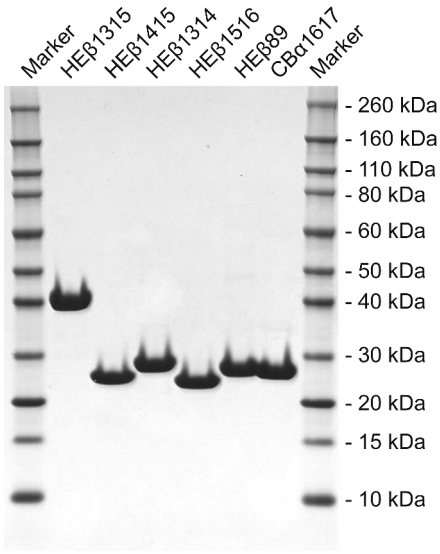

FIGURE 7: Purity and apparent molecular masses of spectrin constructs. A Coomassie Brilliant Blue-stained 4−12% SDS−PAGE gel of the spectrin constructs flanked by molecular mass markers is shown. All fragments were obtained in high yield (5−50 mg/L culture) with >99% purity as determined by SDS−PAGE.

with up to seven extra residues at the N and C termini, the following β-spectrin fragments were cloned, expressed, and purified, as described in the Experimental Procedures: (i) HEβ1314 composed of the 13th and 14th repeats in tandem, (ii) HEβ1415 composed of the 14th and 15th repeats in tandem plus six extra N- and C-terminal residues, (iii) HEβ1516 composed of the 15th and 16th repeats in tandem, and (iv) HEβ1315 composed of the 13−15th repeats in tandem plus two extra N- and C-terminal residues.

The fragments were purified to >99% in high yield as shown by SDS−PAGE (Figure 7). Two-repeat fragments, HEβ89 (*19*) and CBα1617 (*27*), previously characterized by X-ray crystallography are also shown in Figure 7 for comparison.

CD and Fluorescence Spectra Indicate That β-Spectrin Candidates for Ankyrin Binding Are Folded. To demonstrate that all four β-spectrin fragments are well-folded, CD (Figure 8A) and tryptophan fluorescence (Figure 8B) wavelength spectra were measured. Figure 8A shows that all four fragments exhibit the signature α-helical CD profile expected of triple-helical repeats of spectrin (*25*), with troughs at 208 and 222 nm. Their mean residue ellipticities in deg cm^2 dmol^{-1} residue^{-1} and percent α-helical structure, according to a 100% value of 36 000 deg cm^2 dmol^{-1} residue^{-1} (*44*), varied slightly: 31 973 (88.8% α helical) for HEβ1315, 30 188 (83.9% α helical) for HEβ1415, 35 211 (97.8% α helical) for HEβ1314, and 32 894 (91.4% α helical) for HEβ1516. Spectra were also analyzed with a standard secondary-structure analysis algorithm on DICHROWEB, CDDSTR, with reference protein set 3 giving the lowest NRMSDs. All β-spectrin peptides were found to be predominantly α-helical at room temperature: 68% regular α helix and 28% distorted α helix in HEβ1315, 67% regular α helix and 28% distorted α helix in HEβ1415, 67% regular α helix and 26% distorted α helix in HEβ1314, and 68% α helix and 25% distorted α helix in HEβ1516, which are nearly the same as the 67% regular α helix and 28% distorted α helix in HEβ89 and only slightly lower than the 74% regular α helix and 23% distorted α helix in CBα1617. The NRMSD of each fit was <0.01, and the calculated spectra were indistinguishable from experimental spectra (not shown). Figure 8B shows that excitation of tryptophan at 295 nm in all four samples yielded emission spectra with blue-shifted peaks (335 nm for HEβ1315, 336 nm for HEβ1415, 338 nm for HEβ1314, and 338 nm for HEβ1516), as expected of tryptophans shielded within tertiary structure from the bulk phase. Finally, each spectrin fragment was found to fold stably as measured by CD-monitored heat-induced unfolding (included in the Supporting Information).

β-Spectrin Repeats 14 and 15 Are Both Necessary and Sufficient To Form a 1:1 Complex with Zu5 as Demonstrated by Native PAGE. To ascertain the stoichiometry of binding and ensure that the nonbinding of HEβ1314 and HEβ1516 could not be ascribed to their very weak binding to Zu5, the effect of varying the molar ratios of all β-spectrin peptides to Zu5 was examined using native gels (Figure 9). In Figure 9A, nearly all of the HEβ1315 forms a complex with Zu5 at a 1:1 molar ratio. The slight excess of HEβ1315 may indicate a more weakly binding subspecies. At a molar ratio of 1:2, the most slowly migrating free Zu5 appears near the top of the gel and continues to increase in amount as the molar ratio is reduced to 0:1. Likewise, in Figure 9B, nearly all of the HEβ1415 forms a complex with Zu5 at a molar ratio of 1:1, although a very faint excess of HEβ1415 is detectable, perhaps again representing a more weakly binding subspecies. In contrast with parts A and B of Figure 9, Figure 9D of HEβ1516 with Zu5 reveals no complex located between these two proteins at any molar ratio. Figure 9C of HEβ1314 with Zu5 also reveals no complex located between these two proteins at any molar ratio. A 1:1 complex of these spectrin fragments with Zu5 was also found by analytical ultracentrifugation to sedimentation equilibrium (see the Supporting Information).

Affinity and Kinetic Analysis of ABD to Zu5 by SPR. Finally, mutual affinities of the minimal binding domains of these proteins were quantified by SPR (Figure 10). Biotinylated spectrin fragments HEβ1315 (Figure 10A), HEβ1415 (Figure 10B), and CBα1617 were immobilized on separate flow cells of a streptavidin-modified biosensor; Zu5 at various concentrations was then applied over all flow cells simultaneously. For HEβ1315, the average values for the association/dissociation rates and dissociation constant were $k_a = 2.82 \times 10^6 \pm 4.44 \times 10^4$ M^{-1} s^{-1}, $k_d = 4.23 \times 10^{-2} \pm 6.58 \times 10^{-4}$ s^{-1}, and $K_D = 15.0$ nM. Similarly, for HEβ1415, the average values for the association/dissociation rates and dissociation constant were $k_a = 3.61 \times 10^6 \pm 5.70 \times 10^4$ M^{-1} s^{-1}, $k_d = 5.45 \times 10^{-2} \pm 7.46 \times 10^{-4}$ s^{-1}, and $K_D = 15.2$ nM. CBα1617 did not evidence any binding to Zu5 even at higher concentrations; the control shown in Figure 10A corresponds to a Zu5 injection at 1 μM over the CBα1617 flow cell. In all cases, a simple 1:1 binding model with a drifting baseline was used to fit the data. Global reduced χ^2 values ranged from 0.93 to 1.25, indicating good agreement between the modeled fit and the experimental data.

DISCUSSION

Cloned Ankyrin Subdomain Zu5 but Not 272 Forms a Complex with Ankyrin Binding Repeats of Human Erythroid

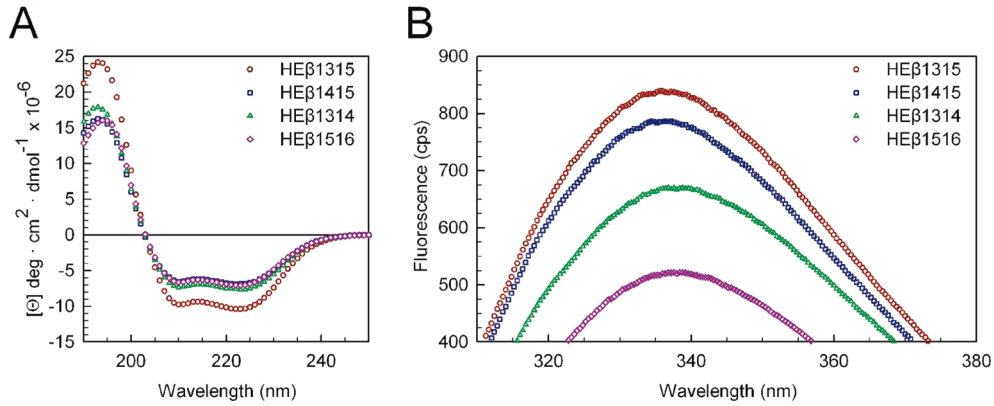

FIGURE 8: CD and tryptophan fluorescence wavelength scans. (A) HEβ1315 (red circles), HEβ1415 (blue squares), HEβ1314 (green triangles), and HEβ1516 (purple diamonds) yield typical α-helical CD spectra, with troughs at 222 and 208 nm. Note that molar ellipticities are given in the graph instead of the mean residue ellipticities reported in the text. (B) Tryptophan emission spectra obtained by excitation at 295 nm exhibit blue-shifted wavelengths of maximum emission ranging from 335 to 338 nm. Intensities reflect the positions of the tryptophans in a repeating heptad pattern described in the Results. Symbols are the same as in A.

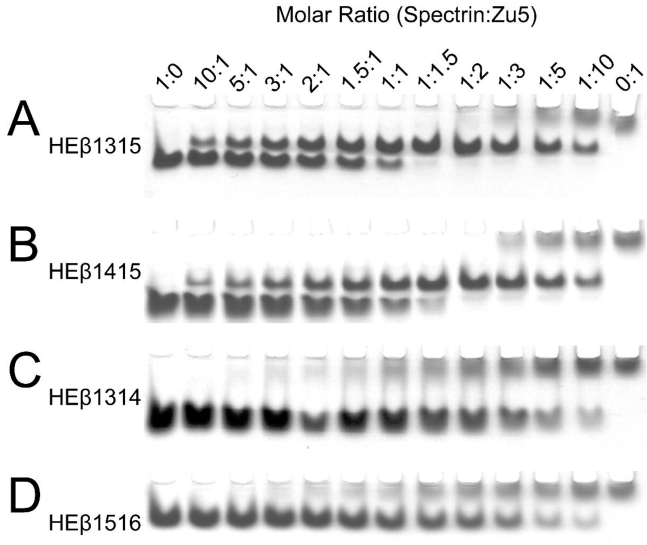

FIGURE 9: Gel-shift assays with varying stoichiometry of spectrin fragments to Zu5 show 1:1 binding. Spectrin fragments and Zu5 mixed in ratios ranging from 1:0 to 0:1 to determine binding stoichiometries. In the case of HEβ1314 and HEβ1516, this assay was performed to rule out the possibility that their binding to Zu5 is weak and could be shifted toward complex formation by adjusting the molar ratios. The two uppermost gels indicate that the spectrin/Zu5 binding ratio is between 1:1 and 1:1.5. When mixed with increasing relative amounts of HEβ1314 but not HEβ1516, Zu5 migration modestly increases; this effect is more prominent in Supplemental Figure S5 in the Supporting Information because of the 5% stacking gel.

β-Spectrin. The 17.6 kDa Zu5 (*16*) but not 10.9 kDa 272 (*15*) of the SpBD of ankyrin (Figure 1) has been shown for the first time to specifically form a complex in a defined system with repeats 14 and 15 and repeats 13−15 of human erythroid β-spectrin by three methods: native PAGE of complexes of spectrin fragments with Zu5 (Figure 5B), nickel-based pull-down assays of His-tagged Zu5 (but not His-tagged 272) bound to β-spectrin fragments (Supplemental Figure S3 in the Supporting Information), and analytical ultracentrifugation to sedimentation equilibrium of complexes of β-spectrin repeats 14 and 15 with Zu5 but not with 272 (Figure 6). Although technical difficulties prevented a straightforward assessment of the inability of 272 to bind to β-spectrin fragments by native PAGE, the results presented here confirm the findings by yeast two-hybrid assays in intact cells (*16, 34*) that Zu5 with its C-terminal neighboring 55 residues (see the Experimental Procedures) is the minimal β-spectrin binding subdomain of ankyrin. In contrast, the results presented here do not confirm the findings by the immunoblot assay of red cell ghost membrane preparations (*15*) that 272 is a β-spectrin-binding subdomain of ankyrin. The purity of ankyrin fragments (Figure 3) and spectrin peptides (Figure 7) cloned for this study makes it unlikely that *in vivo* versus *in vitro* discrepancies can be ascribed to protein contaminants. Previous findings that used undefined sources of binding partners (containing intact spectrin as well as other membrane and nonmembrane proteins) could account for the different outcomes in earlier versus the present work. Perhaps for this reason, it is not uncommon that other interactions of proteins originally detected in undefined systems cannot be confirmed in defined systems (*45*).

Inability To Demonstrate Binding of 272 to HEβ1315 by Native PAGE. As described in the Results and above, it was not possible to show in a straightforward manner by native PAGE alone that 272 does not form a complex with the ankyrin-binding epitope of β-spectrin because either 272 or the spectrin fragments disappeared from the gel during electrophoresis at all pH values tested (e.g., 272 is not seen on the gel in Figure 5A). Apparently the high pI of 272 (9.5) and generally low pI values of spectrin fragments (ranging from 4−6) resulted in their migration to opposite electrodes, so that retention of one peptide species on the gel precluded that of the other. When spectrin fragments were visible on the gel, however, their bands appeared to be of the same intensity and at the same R_f regardless of the presence or absence of 272 in the starting samples. This suggests that none of the spectrin fragments had been lost to a complex with 272. Furthermore, the fact that 272 was not visible when spectrin fragments could be seen in the gel (Figure 5A) rules out precipitation of 272 as a reason for nonbinding. It is also unlikely that the absence of 272−spectrin fragment complexes was due to electric field-induced dissociation during native PAGE, because complexes between β-spectrin fragments and Zu5 (with a nearly equally high pI of 8.5) remained stable.

Self-Aggregation of 272 Is Not Responsible for Its Nonbinding to Spectrin Fragments. The possibility that

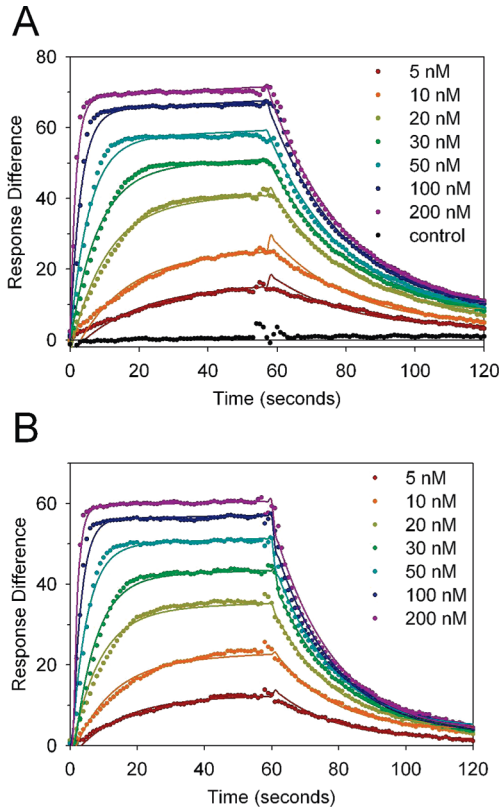

FIGURE 10: SPR determination of binding affinity and kinetics. Representative sensorgrams and fits are shown for the binding of Zu5 to HEβ1315 (A) and HEβ1415 (B) at various concentrations. Data from each concentration series were fit globally and simultaneously for k_a and k_d. The sensorgrams presented reflect the reference and buffer subtracted curves. Zu5 was injected for 60 s, beginning at $t = 0$; an additional 60 s was allowed for dissociation. For HEβ1315 (A), the average values of the three trials were $k_a = 2.82 \times 10^6 \pm 4.44 \times 10^4$ M^{-1} s^{-1}, $k_d = 4.23 \times 10^{-2} \pm 6.58 \times 10^{-4}$ s^{-1}, and $K_D = 15.0$ nM. For HEβ1415 (B), the average values of the three trials were $k_a = 3.61 \times 10^6 \pm 5.70 \times 10^4$ M^{-1} s^{-1}, $k_d = 5.45 \times 10^{-2} \pm 7.46 \times 10^{-4}$ s^{-1}, and $K_D = 15.2$ nM. CBα1617 provided a negative control to demonstrate specific binding, because a 1 μM injection of Zu5 applied over the CBα1617 flow cell resulted in no binding (A, ●). Sensorgrams and fits among the triplicate samples were nearly identical and demonstrated good correspondence between the fit and experimental data, with global reduced χ^2 close to 1.

aggregation of the cloned 272 fragment demonstrated by analytical ultracentrifugation (upper right panel in Figure 6) prevented its binding to spectrin fragments seems unlikely. The K_A of 272 self-aggregation (roughly estimated to be 230 M^{-1} based on analytical ultracentrifugation) is too low to have reduced the 272 monomer level below that required for at least some 272 binding to spectrin fragments. Binding constants of the affinity of spectrin for the SpBD of ankyrin-R lacking 70 of its N-terminal residues have been reported in the 10−200 nM range (*46*). Had 272 bound to β-spectrin fragments, analytical ultracentrifugation to sedimentation equilibrium should have enabled detection of this strength of binding as in the case of cloned β-spectrin repeats 1 and 2 binding to α-spectrin repeats 19 and 20 with K_D values from 20−600 nM (*47*). Finally, although His-tagged Zu5 on Ni−NTA agarose could selectively pull-down β-spectrin repeats 14 and 15 (Supplemental Figure S3A in the Supporting Information), His-tagged 272 was clearly unable to do so (Supplemental Figure S3B in the Supporting Information). Here again, an objection might be made that the His tag on 272 changed its conformation to disallow its binding to the β-spectrin fragments, but because His-tagged Zu5 could bind to the β-spectrin fragments, the suggestion that such a conformational change occurred is unduly speculative.

It should also be noted that repeated attempts were made to demonstrate the interactions between Zu5 or 272 and the β-spectrin repeats 14 and 15 both by CD difference spectra and changes in the sum of the free energies of unfolding of each peptide alone versus that of a mixture of both fragments by procedures reviewed by Greenfield (*48*). Neither strategy was successful (not shown). Attempts to demonstrate binding of 272 to spectrin fragments by these methods were particularly hampered by the tendency of 272 to precipitate despite measurements being performed close to 4 °C.

Both Zu5 and 272 and Their Parent SpBD of Ankyrin Contain Regions That Lack Regular Secondary Structure. A third important new finding in this study is the likely occurrence of substantial intrinsically unstructured regions in Zu5 and 272, according to their CD spectra (Figure 4) and from modeling of their sequences (Supplemental Figure S1 in the Supporting Information) with disordered sequence predictors disEMBL (*49*), GlobPlot (*50*), PONDR (*51, 52*), and DISOPRED2 (*53*). As noted in the Results, the predicted presence of some of the intrinsically unstructured sequences of 272 and Zu5 in their parent spectrin binding domain attests to the context independence of this predicted disorder. For this reason, it is unlikely that these unstructured regions resulted from the sequence design of the cloned fragments.

Having identified Zu5 as the primary β-spectrin-binding domain, we initiated basic nuclear magnetic resonance (NMR) studies to clarify the structural nature of Zu5. Surprisingly, heteronuclear single-quantum coherence (HSQC) data collected with ^{15}N-labeled Zu5 indicated an unexpectedly well-folded protein (Supplemental Figure S2 in the Supporting Information). In the context of the aforementioned CD data and disorder predictions, it seems likely that Zu5 contains little secondary structure yet still adopts a folded conformation. With this finding, carefully differentiating between "unstructured" (folded yet lacking secondary-structure elements) and "disordered" (not adopting a fold) was key to the interpretation of these data. Structural elucidation of the Zu5 subdomain should certainly prove interesting both for its implications for protein folding as well as β-spectrin binding.

Additionally, the content of intrinsically unstructured and/or disordered sequences could have accounted for the limited solubility of Zu5 and 272, although the expression of these protein fragments in bacterial systems unable to glycosylate, fatty acid acylate, or otherwise post-translationally modify may also have contributed to limited solubility. In addition to putative post-translational modifications noted by the website ExPASy, fatty acid acylation of ankyrin has been reported (*54*).

Repeats 14 and 15 of β-Spectrin Are Minimally Necessary and Sufficient To Form Complexes with the Minimal Spectrin Binding Ankyrin. Among fragments of all combinations of phased, well-folded, human erythroid β-spectrin repeats previously implicated in ankyrin binding (*29, 32*), i.e., repeats 13 and 14, repeats 14 and 15, repeats 15 and 16, and repeats 13−15, only fragments containing both repeats 14 and 15 were observed to bind to the Zu5 epitope for β-spectrin.

Native PAGE (Figures 5 and 9), nickel-affinity pull-down assays (Supplemental Figures S3 and S6 in the Supporting Information), and analytical ultracentrifugation to sedimentation equilibrium (Figure 6 and Supplemental Figure S7 in the Supporting Information) results, when taken together, show conclusively that tandem repeats 14 and 15 are necessary and sufficient to bind to the β-spectrin binding site on ankyrin.

CD and Tryptophan Fluorescence Spectra and ΔG Values of Heat-Induced Unfolding Indicate β-Spectrin Fragments Are Similarly Well- and Stably Folded. The CD wavelength spectra of all four β-spectrin fragments in this study exhibit the signature α-helical trace expected for triple-helical bundles (Figure 8). The β-spectrin fragments gave the lowest NRMSD with the CD modeling program CDDSTR (*55*) with reference protein set 6 on DICHROWEB (*42*), yielding 67.5% ± 0.3 regular α helix and 26.8% ± 1.5 distorted α helix. The calculated spectra were indistinguishable from those measured (not shown). The discrepancy between the modeled sum of helical conformations equaling 94% and the helical regions in X-ray crystal structures of repeats equaling 87% (*19, 27, 28*) may reflect the assignment of some loop regions as distorted helix in the latter.

The differences in the tryptophan fluorescence intensities of the fragments (Figure 8B) appear to represent differences in the locations of the tryptophans within a heptad-repeating pattern serving to identify the residues participating in interhelical hydrophobic interactions (*56*). Thus, HEβ16 in HEβ1516 with the lowest fluorescence intensity possesses a tryptophan in an "e" or solvent-exposed position, whereas HEβ13 in HEβ1314 with an intermediate intensity possesses a tryptophan in a "b" or more solvent-protected position. All other tryptophans are in "a" or "d" positions, protected from the solvent and participating in helix-stabilizing, hydrophobic interactions. As expected, these intensities parallel the wavelengths of maximum emission, with the less quenched and therefore more intense spectra being correlated with the lowest wavelengths of maximum emission: 335.6 nm for HEβ1315, 336.4 nm for HEβ1415, 338.8 nm for HEβ1314, and 338.8 nm for HEβ1516. Most importantly, Δ*G* values of heat-induced unfolding monitored by CD were nearly the same for all β-spectrin peptides, as shown in heat-denaturation curves in Supplemental Figure S4 in the Supporting Information. Hence, nonbinding to Zu5 of spectrin fragments without repeats 14 or 15 (i.e., HEβ1516 or HEβ1314) cannot be attributed to relative instability of folding of those fragments.

1:1 Stoichiometry of Binding of β-Spectrin Repeats to Ankyrin Subdomain Zu5 by Native PAGE. Not only did native PAGE demonstrate the binding of β-spectrin repeats 14 and 15 and 13−15 to Zu5 (Figure 5), this method was also a convenient way of demonstrating near 1:1 stoichiometry (parts A and B of Figure 9). In addition, binding did not occur between Zu5 and the "incomplete" ankyrin binding domain fragments HEβ1314 and HEβ1516, even at a spectrin/Zu5 ratio of 10:1 (parts C and D of Figure 9, respectively). Thus, HEβ1314 and HEβ1516 appeared to be entirely inactive in binding to Zu5 and not merely weakly binding. However, although no freely migrating complex with HEβ1314 is observed in Figure 9C, careful inspection of Supplemental Figure S5 in the Supporting Information reveals that at 1:1 HEβ1314 is almost imperceptibly retarded in its mobility, whereas Zu5 has migrated slightly faster. This result is highly reproducible and easily discerned when a 5% stacking gel is used. These slight differences in the extent of migration during electrophoresis could signify conformational changes occurring upon interaction of Zu5 with HEβ14, which are necessary but not sufficient for stable complex formation.

Kinetic and Affinity Measurements of β-Spectrin Fragments to Zu5. SPR binding measurements of Zu5 to biotinylated spectrins validated the results of many of the aforementioned studies while also providing quantitative kinetic and affinity measurements. Zu5 binding was again found to be specific to repeats 14 and 15 with 1:1 stoichiometry, because there was no binding to CBα1617 (● in Figure 10A). Interestingly, comparisons of Zu5 binding to HEβ1315 (Figure 10A) versus HEβ1415 (Figure 10B) exhibited very slight differences in binding kinetics with no appreciable change in K_D (15.2 versus 15.0 nM, respectively). This was somewhat surprising because additional spectrin repeats are known to stabilize spectrin fragments (*33*) yet did not have an impact on SpBD binding affinity. Additionally, the reasonably strong binding of these fragments was slightly tighter than expected on the basis of studies of intact spectrin and ankyrin [∼25 nM (*35*)], suggesting that these minimal regions may be responsible for nearly all of the binding affinity.

In conclusion, these binding epitopes of ankyrin and β-spectrin continue to present a host of tantalizing questions, most recently with respect to dysfunction in lateral membrane biogenesis and abnormal distributions of membrane proteins in various cell types because of mutations of polar to alanine residues within the SpBD without an apparent effect on ankyrin folding (*34*). The possibility that those mutated residues occupy sites of ankyrin−β-spectrin interaction calls for testing in the type of defined system amenable to structural analysis, which has been presented here. A second major question is whether the regions of SpBD, which lack secondary structure, might eventually undergo folding upon interacting with ankyrin binding epitopes or other function-determining sites of β-spectrin. A number of such intrinsically unstructured regions do fold upon meeting their binding partners (*57*), whereas others persist and function in an unstructured state (*58*). After many years of intense study of protein folding, a new era is literally and figuratively unfolding, so that alternative paradigms may provide greater understanding of the relationship between the structure and function of proteins with intrinsically unstructured regions, such as the β-spectrin binding domain of ankyrin.

In view of the finding by Winograd et al. (*30*) that cloning of well-folded spectrin repeats required their being "phased" or consisting of integral, nonfractional numbers of repeats, the binding activity of "unphased" repeats might be considered to be of dubious physiological significance. Nevertheless, the results presented here on "phased" repeats agree well with those on "unphased" repeats by Kennedy et al. (*29*) and Hryniewicz-Jankowska et al. (*32*), insofar as the former identified the C-terminal third of β-spectrin repeat 14 and the whole of repeat 15 and the latter found a fragment from repeat 13 to the middle of repeat 15 to be the spectrin binding site on ankyrin. Upon closer inspection of ref *32*, however, the minimal "phased" region of maximal binding consisted of only β-spectrin repeats 14 and 15 with no kinetic

or thermodynamic advantage evidenced by inclusion of β-spectrin repeat 13.

Now that a defined system of well-folded peptides is available for structural study of the interactions between the minimal β-spectrin-binding domain of ankyrin and the minimal ankyrin-binding domain of β-spectrin, we hope to characterize the β-spectrin/ankyrin-binding interface comprising the C-terminal third of β-spectrin repeat 14 and the N-terminal half of β-spectrin repeat 15 at the molecular level. Interest in this interface has been heightened by the recent finding of the force-induced accessibility of the single cysteine in repeat 15 of β-spectrin to IAEDANS labeling in intact red cells (*59*).

ACKNOWLEDGMENT

We thank Dr. Bernard Forget for cDNA of human erythroid β-spectrin and Dr. Patrick Gallagher for the cDNA of human erythroid ankyrin, Dr. Francis Neuhaus and the laboratory of Dr. Thomas J. Meade for the use of equipment, the staff of the Keck Biophysics Facility at Northwestern University for instrument support, Dr. Ishwar Radhakrishnan and his laboratory for assistance with NMR experiments, Sarah Maar for help with cloning and expression with pMCSG7, Drs. Alfonso Mondragón and Robert C. MacDonald for fruitful discussions, and Carrie Clendaniel, Kai Huang, Amy Anichini, Ang Li, and Andrew Chang for laboratory assistance. The authors gratefully acknowledge the use of instruments in the Chemistry Core at the Institute for BioNanotechnology in Medicine at Northwestern University, which is partly supported by NIH award 5P50NS054287. J.J.I. especially thanks Chung-Yan Koh in the laboratory of Dr. Samuel Stupp for instrument access and assistance with ESI−MS and Dr. Elena Solomaha of the Biophysics Core Facility at the University of Chicago for guidance, suggestions, and encouragement with SPR experiments.

SUPPORTING INFORMATION AVAILABLE

Supplemental Experimental Methods; Supplemental Results; Supplemental Discussion; Supplemental Figure S1, prediction of intrinsic disorder in Zu5 and 272; Supplemental Figure S2, HSQC spectrum of ^{15}N-labeled Zu5 reveals a surprisingly well-folded protein; Supplemental Figure S3, nickel pull-down assay with His-tagged Zu5 but not His-tagged 272 indicates binding to HEβ1415; Supplemental Figure S4, HEβ1314, HEβ1415, and HEβ1516 are stably folded on heat denaturation monitored by CD; Supplemental Figure S5, gel-shift assay with Zu5 implicates HEβ1415 as minimal binding repeats; Supplemental Figure S6, nickel pull-down assay with His-tagged Zu5 confirms HEβ1415 as minimally necessary for binding; and Supplemental Figure S7, analytical ultracentrifugation to sedimentation equilibrium indicates Zu5 stably binds to HEβ1415. This material is available free of charge via the Internet at http://pubs.acs.org.

REFERENCES

1. Mohandas, N., and Evans, E. (1994) Mechanical properties of the red cell membrane in relation to molecular structure and genetic defects. *Annu. Rev. Biophys. Biomol. Struct. 23*, 787–818.
2. Tse, W. T., and Lux, S. E. (1999) Red blood cell membrane disorders. *Br. J. Hamaetol. 104*, 2–13.
3. Gimm, J. A., An, X., Nunomura, W., and Mohandas, N. (2002) Functional characterization of spectrin−Actin-binding domains in 4.1 family of proteins. *Biochemistry 41*, 7275–7282.
4. Bennett, V. (1992) Ankyrins. Adaptors between diverse plasma membrane proteins and the cytoplasm. *J. Biol. Chem. 267*, 8703–8706.
5. Chang, S. H., and Low, P. S. (2001) Regulation of the glycophorin C-protein 4.1 membrane-to-skeleton bridge and evaluation of its contribution to erythrocyte membrane stability. *J. Biol. Chem. 276*, 22223–22230.
6. Tomishige, M., Sako, Y., and Kusumi, A. (1998) Regulation mechanism of the lateral diffusion of band 3 in erythrocyte membranes by the membrane skeleton. *J. Cell Biol. 142*, 989–1000.
7. Bennett, V., and Baines, A. J. (2001) Spectrin and ankyrin-based pathways: Metazoan inventions for integrating cells into tissues. *Physiol. Rev. 81*, 1353–1392.
8. Ogawa, Y., Schafer, D. P., Horresh, I., Bar, V., Hales, K., Yang, Y., Susuki, K., Peles, E., Stankewich, M. C., and Rasband, M. N. (2006) Spectrins and ankyrinB constitute a specialized paranodal cytoskeleton. *J. Neurosci. 26*, 5230–5239.
9. Anong, W. A., Weis, T. L., and Low, P. S. (2006) Rate of rupture and reattachment of the band 3-ankyrin bridge on the human erythrocyte membrane. *J. Biol. Chem. 281*, 22360–22366.
10. Cunha, S. R., and Mohler, P. J. (2006) Cardiac ankyrins: Essential components for development and maintenance of excitable membrane domains in heart. *Cardiovasc. Res. 71*, 22–29.
11. Bennett, V., and Healy, J. (2007) Organizing the fluid membrane bilayer: Diseases linked to spectrin and ankyrin. *Trends Mol. Med. 13*, 13.
12. Michaely, P., Tomchick, D. R., Machius, M., and Anderson, R. G. (2002) Crystal structure of a 12 ANK repeat stack from human ankyrinR. *EMBO J. 21*, 6387–6396.
13. Lee, G., Abdi, K., Jiang, Y., Michaely, P., Bennett, V., and Marszalek, P. E. (2006) Nanospring behaviour of ankyrin repeats. *Nature 440*, 246–249.
14. Wallin, R., Culp, E. N., Coleman, D. B., and Goodman, S. R. (1984) A structural model of human erythrocyte band 2.1: Alignment of chemical and functional domains. *Proc. Natl. Acad. Sci. U.S.A. 81*, 4095–4099.
15. Platt, O. S., Lux, S. E., and Falcone, J. F. (1993) A highly conserved region of human erythrocyte ankyrin contains the capacity to bind spectrin. *J. Biol. Chem. 268*, 24421–24426.
16. Mohler, P. J., Yoon, W., and Bennett, V. (2004) Ankyrin-B targets β2-spectrin to an intracellular compartment in neonatal cardiomyocytes. *J. Biol. Chem. 279*, 40185–40193.
17. Zhang, J., Xu, L. G., Han, K. J., and Shu, H. B. (2004) Identification of a ZU5 and death domain-containing inhibitor of NF-κB. *J. Biol. Chem. 279*, 17819–17825.
18. Evans, E. A., and Skalak, R. (1979) Mechanics and thermodynamics of biomembranes. *CRC Crit. Rev. Bioeng. 3*, 181–330.
19. Kusunoki, H., MacDonald, R. I., and Mondragón, A. (2004) Structural insights into the stability and flexibility of unusual erythroid spectrin repeats. *Structure 12*, 645–656.
20. MacDonald, R. I., and Cummings, J. A. (2004) Stabilities of folding of clustered, two-repeat fragments of spectrin reveal a potential hinge in the human erythroid spectrin tetramer. *Proc. Natl. Acad. Sci. U.S.A. 101*, 1502–1507.
21. An, X., Guo, X., Zhang, X., Baines, A. J., Debnath, G., Moyo, D., Salomao, M., Bhasin, N., Johnson, C., Discher, D., Gratzer, W. B., and Mohandas, N. (2006) Conformational stabilities of the structural repeats of erythroid spectrin and their functional implications. *J. Biol. Chem. 281*, 10527–10532.
22. Djinovic-Carugo, K., Gautel, M., Ylanne, J., and Young, P. (2002) The spectrin repeat: A structural platform for cytoskeletal protein assemblies. *FEBS Lett. 513*, 119–123.
23. Byers, T. J., Brandin, E., Lue, R. A., Winograd, E., and Branton, D. (1992) The complete sequence of *Drosophila* β-spectrin reveals supra-motifs comprising eight 106-residue segments. *Proc. Natl. Acad. Sci. U.S.A. 89*, 6187–6191.
24. Broderick, M. J., and Winder, S. J. (2005) Spectrin, α-actinin, and dystrophin. *Adv. Protein Chem. 70*, 203–246.
25. Speicher, D. W., and Marchesi, V. T. (1984) Erythrocyte spectrin is comprised of many homologous triple helical segments. *Nature 311*, 177–180.
26. Djinovic-Carugo, K., Young, P., Gautel, M., and Saraste, M. (1999) Structure of the α-actinin rod: Molecular basis for cross-linking of Actin filaments. *Cell 98*, 537–546.

27. Grum, V. L., Li, D., MacDonald, R. I., and Mondragón, A. (1999) Structures of two repeats of spectrin suggest models of flexibility. *Cell 98*, 523–535.
28. Kusunoki, H., Minasov, G., MacDonald, R. I., and Mondragón, A. (2004) Independent movement, dimerization and stability of tandem repeats of chicken brain α-spectrin. *J. Mol. Biol. 344*, 495–511.
29. Kennedy, S. P., Warren, S. L., Forget, B. G., and Morrow, J. S. (1991) Ankyrin binds to the 15th repetitive unit of erythroid and nonerythroid β-spectrin. *J. Cell Biol. 115*, 267–277.
30. Winograd, E., Hume, D., and Branton, D. (1991) Phasing the conformational unit of spectrin. *Proc. Natl. Acad. Sci. U.S.A. 88*, 10788–10791.
31. Stabach, P. R., and Morrow, J. S. (2000) Identification and characterization of βV spectrin, a mammalian ortholog of *Drosophila* βH spectrin. *J. Biol. Chem. 275*, 21385–21395.
32. Hryniewicz-Jankowska, A., Bok, E., Dubielecka, P., Chorzalska, A., Diakowski, W., Jezierski, A., Lisowski, M., and Sikorski, A. F. (2004) Mapping of an ankyrin-sensitive, phosphatidylethanolamine/phosphatidylcholine mono- and bi-layer binding site in erythroid β-spectrin. *Biochem. J. 382*, 677–685.
33. MacDonald, R. I., and Pozharski, E. V. (2001) Free energies of urea and of thermal unfolding show that two tandem repeats of spectrin are thermodynamically more stable than a single repeat. *Biochemistry 40*, 3974–3984.
34. Kizhatil, K., Yoon, W., Mohler, P. J., Davis, L. H., Hoffman, J. A., and Bennett, V. (2007) Ankyrin-G and β2-spectrin collaborate in biogenesis of lateral membrane of human bronchial epithelial cells. *J. Biol. Chem. 282*, 2029–2037.
35. Davis, J. Q., and Bennett, V. (1984) Brain ankyrin. A membrane-associated protein with binding sites for spectrin, tubulin, and the cytoplasmic domain of the erythrocyte anion channel. *J. Biol. Chem. 259*, 13550–13559.
36. Gallagher, P. G., Tse, W. T., Scarpa, A. L., Lux, S. E., and Forget, B. G. (1997) Structure and organization of the human ankyrin-1 gene. Basis for complexity of pre-mRNA processing. *J. Biol. Chem. 272*, 19220–19228.
37. Lambert, S., Yu, H., Prchal, J. T., Lawler, J., Ruff, P., Speicher, D., Cheung, M. C., Kan, Y. W., and Palek, J. (1990) cDNA sequence for human erythrocyte ankyrin. *Proc. Natl. Acad. Sci. U.S.A. 87*, 1730–1734.
38. Winkelmann, J. C., Chang, J. G., Tse, W. T., Scarpa, A. L., Marchesi, V. T., and Forget, B. G. (1990) Full-length sequence of the cDNA for human erythroid β-spectrin. *J. Biol. Chem. 265*, 11827–11832.
39. Wasenius, V. M., Saraste, M., Salven, P., Eramaa, M., Holm, L., and Lehto, V. P. (1989) Primary structure of the brain α-spectrin [published erratum appears in *J. Cell Biol.* (1989) Mar *108* (3) following 1175]. *J. Cell Biol. 108*, 79–93.
40. Stols, L., Gu, M., Dieckman, L., Raffen, R., Collart, F. R., and Donnelly, M. I. (2002) A new vector for high-throughput, ligation-independent cloning encoding a tobacco etch virus protease cleavage site. *Protein Expression Purif. 25*, 8–15.
41. Sambrook, J., Fritsch, E. F., and Maniatis, T. (1989) *Molecular Cloning: A Laboratory Manual*, 2nd ed., Cold Spring Harbor Laboratory Press, Cold Spring Harbor, NY.
42. Whitmore, L., and Wallace, B. A. (2004) DICHROWEB, an online server for protein secondary structure analyses from circular dichroism spectroscopic data. *Nucleic Acids Res. 32*, W668–W673.
43. Sreerama, N., Venyaminov, S. Y., and Woody, R. W. (2000) Estimation of protein secondary structure from circular dichroism spectra: Inclusion of denatured proteins with native proteins in the analysis. *Anal. Biochem. 287*, 243–251.
44. Greenfield, N., and Fasman, G. D. (1969) Computed circular dichroism spectra for the evaluation of protein conformation. *Biochemistry 8*, 4108–4116.
45. Sánchez-Puig, N., Veprintsev, D. B., and Fersht, A. R. (2005) Human full-length securin is a natively unfolded protein. *Protein Sci. 14*, 1410–1418.
46. Davis, L. H., and Bennett, V. (1990) Mapping the binding sites of human erythrocyte ankyrin for the anion exchanger and spectrin. *J. Biol. Chem. 265*, 10589–10596.
47. Harper, S. L., Begg, G. E., and Speicher, D. W. (2001) Role of terminal nonhomologous domains in initiation of human red cell spectrin dimerization. *Biochemistry 40*, 9935–9943.
48. Greenfield, N. J. (2004) Circular dichroism analysis for protein−protein interactions. *Methods Mol. Biol. 261*, 55–78.
49. Linding, R., Jensen, L. J., Diella, F., Bork, P., Gibson, T. J., and Russell, R. B. (2003) Protein disorder prediction: Implications for structural proteomics. *Structure 11*, 1453–1459.
50. Linding, R., Russell, R. B., Neduva, V., and Gibson, T. J. (2003) GlobPlot: Exploring protein sequences for globularity and disorder. *Nucleic Acids Res. 31*, 3701–3708.
51. Romero, P., Obradovic, Z., Kissinger, C., Villafranca, J. E., Dunker, A. K. (1997) In International Conference on Neural Networks, pp 90−95, Houston, TX.
52. Vucetic, S., Brown, C. J., Dunker, A. K., and Obradovic, Z. (2003) Flavors of protein disorder. *Proteins 52*, 573–584.
53. Ward, J. J., Sodhi, J. S., McGuffin, L. J., Buxton, B. F., and Jones, D. T. (2004) Prediction and functional analysis of native disorder in proteins from the three kingdoms of life. *J. Mol. Biol. 337*, 635–645.
54. Staufenbiel, M., and Lazarides, E. (1986) Ankyrin is fatty acid acylated in erythrocytes. *Proc. Natl. Acad. Sci. U.S.A. 83*, 318–322.
55. Sreerama, N., and Woody, R. W. (2000) Estimation of protein secondary structure from circular dichroism spectra: Comparison of CONTIN, SELCON, and CDSSTR methods with an expanded reference set. *Anal. Biochem. 287*, 252–260.
56. Parry, D. A., Dixon, T. W., and Cohen, C. (1992) Analysis of the three-α helix motif in the spectrin superfamily of proteins. *Biophys. J. 61*, 858–867.
57. Radhakrishnan, I., Perez-Alvarado, G. C., Dyson, H. J., and Wright, P. E. (1998) Conformational preferences in the Ser133-phosphorylated and non-phosphorylated forms of the kinase inducible transactivation domain of CREB. *FEBS Lett. 430*, 317–322.
58. Konno, T., Tanaka, N., Kataoka, M., Takano, E., and Maki, M. (1997) A circular dichroism study of preferential hydration and alcohol effects on a denatured protein, pig calpastatin domain I. *Biochim. Biophys. Acta 1342*, 73–82.
59. Johnson, C. P., Tang, H. Y., Carag, C., Speicher, D. W., and Discher, D. E. (2007) Forced unfolding of proteins within cells. *Science 317*, 663–666.
60. Kabsch, W., and Sander, C. (1983) Dictionary of protein secondary structure: Pattern recognition of hydrogen-bonded and geometrical features. *Biopolymers 22*, 2577–2637.

BI702525Z